Published in final edited form as:
J Immunol. 2011 January 1; 186(1): 621–631. doi:10.4049/jimmunol.1002230.

Autoimmune Kidney Disease and Impaired Engulfment of Apoptotic Cells in Mice with Macrophage Peroxisome Proliferator-Activated Receptor γ or Retinoid X Receptor α Deficiency

Tamás Rőszer[*,1], **María P. Menéndez-Gutiérrez**[*,1], **Martina I. Lefterova**[†,‡,§], **Daniel Alameda**[*], **Vanessa Núñez**[*], **Mitchell A. Lazar**[†,‡,§], **Thierry Fischer**[¶], and **Mercedes Ricote**[*]

[*]Departamento de Cardiología Regenerativa, Centro Nacional de Investigaciones Cardiovasculares, 28029 Madrid, Spain

[¶]Departamento de Inmunología y Oncología, Centro Nacional de Biotecnología, Consejo Superior de Investigaciones Científicas, 28049 Madrid, Spain

[†]Division of Endocrinology, Diabetes and Metabolism, Department of Medicine, University of Pennsylvania School of Medicine, Philadelphia, PA 19104

[‡]Department of Genetics, University of Pennsylvania School of Medicine, Philadelphia, PA 19104

[§]Institute for Diabetes, Obesity and Metabolism, University of Pennsylvania School of Medicine, Philadelphia, PA 19104

Abstract

Autoimmune glomerulonephritis is a common manifestation of systemic lupus erythematosus (SLE). In this study, we show that mice lacking macrophage expression of the heterodimeric nuclear receptors PPARγ or RXRα develop glomerulonephritis and autoantibodies to nuclear Ags, resembling the nephritis seen in SLE. These mice show deficiencies in phagocytosis and clearance of apoptotic cells, and they are unable to acquire an anti-inflammatory phenotype upon feeding of apoptotic cells, which is critical for the maintenance of self-tolerance. These results demonstrate that stimulation of PPARγ and RXRα in macrophages facilitates apoptotic cell engulfment, and they provide a potential strategy to avoid autoimmunity against dying cells and to attenuate SLE.

Systemic lupus erythematosus (SLE) is an autoimmune disorder that can present with a renal involvement that leads to SLE nephritis (1). SLE nephritis develops as a consequence of autoreactive B cell activation, production and intrarenal deposition of autoantibodies and

Address correspondence and reprint requests to Mercedes Ricote, Centro Nacional de Investigaciones Cardiovasculares, Melchor Fernández Almagro 3, 28029 Madrid, Spain. mricote@cnic.es.

[1]T.R. and M.P.M-G. contributed equally to this work.

The online version of this article contains supplemental material.

Disclosures

The authors have no financial conflicts of interest.

complement components, macrophage activation, and the generation of proinflammatory cytokines. SLE nephritis disrupts renal function, contributes to the development of peripheral vascular disease, and increases the risk of cardiovascular mortality (2).

The disease mechanism of SLE was shown recently to involve impaired clearance of apoptotic cells, which has led to a conceptual change in our understanding of the disease (3). The nuclear DNA fragments and nuclear proteins of dying cells are self-Ags, and they are important triggers of autoreactive Ig production (4). The safe removal of apoptotic cell debris is a dedicated function of phagocytic cells, particularly tissue-resident macrophages (5, 6). Signals from apoptotic cells direct the activation of macrophages toward a so-called regulatory or deactivated phenotype, thereby dampening inflammation (7–9). Macrophages reprogrammed by apoptotic cells control and deactivate immunity and inflammation by triggering the release of anti-inflammatory cytokines, such as TGF-β and IL-10, and inhibiting the production of proinflammatory cytokines. In pathologies in which apoptotic cell clearance is disrupted, as in SLE, the absence of this suppressive effect on inflammatory cytokine production by macrophages could aggravate chronic inflammation (10). To correctly engulf apoptotic cells, macrophages express a large set of cell surface receptors, including scavenger receptors (e.g., CD36, CD14), integrins (e.g., ITGA5, ITGB3), Ig supergene family receptors (e.g., FcγRs), receptors for complement factors (e.g., LRP1/Calr, the low-density lipoprotein receptor-related protein 1/calreticulin complex), complement receptor 3 (CR3, also known as ITGM), complement receptor 4 (CR4, also known as ITGX), and Tyro3/Axl/Mertk (TAM) family tyrosine kinase cell surface receptor. Apoptotic cell removal is enhanced by bridging molecules (opsonins), which interact with macrophage receptors and apoptotic cell molecules. Opsonins include components of the complement system (C1q, C3b, C4b, and iC3b), immunoglobulins (IgG and IgM), MFG-E8, THBS1, and GAS6. Altered expression of some cell-surface receptors and opsonins has been proposed to influence the development of SLE (11–13).

Ligands of peroxisome proliferator activated receptor γ (PPARγ) modulate macrophage function and regulate the expression of a range of inflammatory genes, making them potential drugs for the treatment of inflammation and immune responses (14). Activators of PPARγ include lipid metabolites and synthetic thiazolidinediones such as rosiglitazone (RSG) (15). PPARγ belongs to the nuclear receptor superfamily of ligand-dependent transcription factors and affects various cellular processes at the level of gene expression regulation (16, 17). PPARγ controls macrophage polarization and inhibits expression of inflammatory genes (14); therefore, it is a key regulator of macrophage-mediated immune responses (15, 18). PPARγ forms a permissive heterodimer with retinoid X receptors (RXRs). These nuclear receptors, encoded by three distinct genes (*Rxra*, *Rxrb*, *Rxrg*), are heterodimer-forming partners of other nuclear receptors (19). The most important RXR isoform in macrophages is RXRα (20), which is activated by its natural ligand 9-*cis*-retinoic acid (9cRA) and by the synthetic ligand LG268 (21). Permissive PPARγ/RXRα heterodimers can be activated by ligands of either receptor and have additive or synergistic downstream effects, suggesting that PPARγ might modulate macrophage functions through heterodimerization with RXRα (16, 19, 22, 23). However, the immunomodulatory role of PPARγ/RXRα heterodimers in macrophages is still un-defined.

In this study, we show that macrophage-specific deletion of PPARγ or RXRα leads to glomerular damage and an elevated production of autoantibodies to nuclear Ags, both hallmarks of SLE. Mice lacking macrophage PPARγ or RXRα show impaired engulfment of apoptotic cells and a deficient expression of a gene network implicated in phagocytosis. These results indicate that PPARγ and RXRα signaling in macrophages is essential for the efficient clearance of apoptotic cells and the maintenance of self-tolerance, an important element of tissue homeostasis and a mechanism disrupted in SLE. The impaired uptake of apoptotic cells by macrophages is an initiator of autoimmunity, making macrophage PPARγ and RXRα candidate targets for new SLE medication strategies (1).

Materials and Methods

Animals

Mice carrying floxed alleles of PPARγ (PPARγ$^{f/f}$) or RXRα (RXRα$^{f/f}$) were generated as described previously (18, 24). We used a conditional knockout (KO) mouse model with myeloid-specific PPARγ ablation to generate mice lacking macrophage PPARγ or RXRα (20). Mice bearing the lox-P-targeted PPARγ (PPARγ$^{f/f}$) or RXRα (RXRα$^{f/f}$) allele and the lysozyme-M Cre (LysMCre) recombinase transgene were crossed to generate offspring with macrophage-specific loss of the PPARγ or RXRα gene. We refer to LysMCre-negative PPARγ$^{f/f}$ and RXRα$^{f/f}$ mice as wild type (WT), and their PPARγ$^{f/f}$LysMCre^{+} or RXRα$^{f/f}$LysMCre^{+} littermates as knockout animals (PPARγ-KO and RXRα-KO). All mice were on a 129/Sv and C57BL/6 background. Female mice aged 4–6 or 14–16 mo were used for experiments. Mice were genotyped by PCR (18). Experiments were performed according to local ethical guidelines and were approved by the Animal Subjects Committee of the Instituto Carlos III (Madrid, Spain) in accordance with EU Directive 86/609/EEC. Mice were killed by CO_2 inhalation.

Optical projection tomographic, histologic, and ultrastructural analysis of kidney

To characterize glomerular angioarchitecture, kidneys were perfused with water resistant ink through the renal arteries and immediately fixed in 10% paraformaldehyde (PFA) diluted in PBS (0.1 M, pH 7.4) for 24 h. Samples were prepared for optical projection tomography (OPT) by a processing protocol that provides high tissue transparency to allow scanning of arterial casts (25). OPT was performed with a Bioptonics Microscopy OPT Scanner 3001 (Bioptonics, Edinburgh, Scotland).

For histologic analysis, kidneys were dissected, weighed, and fixed in 4% PFA for 24 h. Tissues were dehydrated, cleared in xylene, and finally embedded in Paraplast embedding medium (Structure Probe, West Chester, PA). Microtome sections (5 μm) were stained with Harris H&E or periodic acid-Schiff (PAS) according to the manufacturer's protocol (Sigma-Aldrich, St, Louis, MO). Glomerular diameter and the number of glomerular cell nuclei were determined by histomorphometric analysis of digital images taken at ×400 magnification according to a previously described method (26). Apoptotic cells were labeled with either the TUNEL Apoptag Plus Peroxidase Kit (Chemicon, Temecula, CA) or the In Situ Cell Death Detection Kit (Roche, Basel, Switzerland), or they were immunostained for cleaved caspase 3 (Cell Signaling Technology, Beverly, MA). The apoptotic index, the

percentage of TUNEL positive nuclei in glomeruli, was calculated from counts of more than 60 glomeruli per sample. For silver impregnation of basement membranes, we used the PAS-methenamine-silver method (IHC Worldwide). Immunostainings for mouse F4/80 (Abcam, Cambridge, U.K.), CD68 (Santa Cruz Biotechnology, Santa Cruz, CA), vascular endothelial growth factor-A (VEGF-A; Abcam), TNFα (Santa Cruz Biotechnology), inducible NO synthase (iNOS; Santa Cruz Biotechnology), and IL-10 and IL1β (Abcam) were performed on vibratome sections following the manufacturer's protocols. For visualization, we used the Vectastain ABC Elite Universal Kit (Vector Laboratories, Burlingame, CA). Distribution of mouse IgG and IgM was determined by Fab-specific anti-mouse IgG and μ-specific anti-mouse IgM (27) (FITC conjugated, developed in goat; Sigma-Aldrich).

For analysis of cell ultrastructure, samples were cut from the kidney cortex and immersed immediately in a mixture of PFA and glutaraldehyde (4/1). Samples were dehydrated and embedded in Durcupan resin (Sigma-Aldrich). Semithin sections were osmificated and uranyl acetate contrasted, and finally ultrathin sections were mounted on grids and examined with a JEOL JEM 1010 transmission electron microscope. Images were taken with a Sony digital camera.

Clinical chemistry

Animals were kept individually in metabolic chambers (Tecniplast, Italy) and urine samples were pooled over 24 h. Total urinary albumin was determined by latex turbidimetry (Turbilatex; Spinreact; Sant Esteve d'en Bas, Spain). Serum creatinine was measured from tail vein blood samples by an enzymatic endpoint colorimetric method (Spinreact). Measurements were recorded with a Spinlab 100 clinical chemistry analyzer (Spinreact, Girona, Spain). Urinary proteins were separated by continuous 12% SDS-PAGE. Serum VEGF-A was measured with a mouse VEGF-A ELISA kit (Bender MedSystems, Vienna, Austria), and serum titers of autoreactive Abs (anti-ssDNA, anti-dsDNA and anti-nuclear Ab [ANA]) were determined with an ELISA kit (αDiagnostics, San Antonio, TX).

Flow cytometry

Cell suspensions were prepared from spleen, axillary and neck lymph nodes, and freshly harvested femur bone marrow from WT, PPARγ-KO, and RXRα KO mice. The cells were analyzed by FACS. The following labeled Abs were used to detect different leukocyte subpopulations: FITC-labeled anti–c-Kit and anti-IgM, PE-labeled anti-Ly6G and anti-CD4, Alexa Fluor 647-labeled anti-Cd11b and B220, Alexa Fluor 488-labeled Ly6C and CD3, PE-Cy7–labeled anti-F4/80, Pacific Blue-labeled anti-CD45, allo-phycocyanin-labeled anti–SCA-1, PerCP-labeled anti-CD8, and biotin-conjugated Lin. Cells were analyzed with a FACSCalibur flow cytometer and CellQuest software (BD Biosciences, San Jose, CA).

Preparation of apoptotic thymocytes

Apoptotic thymocytes (ATs) were generated and fluorescently labeled as described (28). Thymocytes were harvested from 4-wk-old C57BL/6 mice. Cells were treated with 1 μM dexamethasone (Sigma-Aldrich) for 6 h at 37°C and were then FITC-labeled with CellTracker green (Invitrogen, Carlsbad, CA). Efficient induction of apoptosis was

confirmed by flow cytometry using the Annexin-FITC Apoptosis Detection Kit (BD Pharmingen, San Diego, CA). Dexamethasone treatment yielded an AT population with ~70% apoptotic cells (Supplemental Fig. 2*A*).

Analysis of apoptotic cell clearance in vivo

Fluorescently labeled ATs (2×10^6) were injected i.p. into WT, RXRα-KO, or PPARγ-KO mice. Animals were sacrificed after 6 or 14 h, peritoneal cells were retrieved by lavage, and free ATs were examined with a Leica AM TIRF MC wide field fluorescent-differential interference contrast microscope (Leica Microsystems, Deerfield, IL) and counted with a hemocytometer. For ultrastructural analysis, macrophages retrieved by lavage were pooled in 5% agar gel, fixed in a mixture of PFA and glutaraldehyde (4/1), and processed for electron microscopy as described above.

Analysis of phagocytosis of apoptotic cells and opsonized RBCs

The phagocytosis assay was performed as described previously (29). Peritoneal exudates were collected by lavage from mice treated with 3% thioglycollate 3 d before cell isolation. The macrophage cell population was obtained after negative selection with magnetic bead-conjugated rat anti-mouse Ly-6G Ig (eBioscience, San Diego, CA). Cells were plated on coverslips in 24-well culture plates in RPMI 1640 medium supplemented with 2% FBS (Life Technologies, Rockville, MD) and penicillin-streptomycin. To test the effects of PPARγ and RXRα ligands, macrophages were treated for 18 h with 1μM RSG (Cayman Chemical, Ann Arbor, MI) or 100 nM 9cRA (Sigma-Aldrich). Before the phagocytosis assay, macrophages were starved for 2 h in RPMI 1640 containing 20 mM Hepes, L-glutamine, and penicillin-streptomycin. ATs were added to macrophages at a 5:1 ratio and incubated for 1 h. Wells were washed five times with PBS and cells were fixed with 1% PFA. Coverslips were mounted with Prolong Gold antifade reagent containing DAPI (Invitrogen; Molecular Probes, Eugene, OR). RBCs from sheep blood (Cappel, ICN Pharmaceuticals, London, U.K.) were suspended in PBS containing 20 mM glucose and mixed 1:10 with anti-sheep RBC IgG (Cappel) or 1:7 with anti-sheep RBC IgM (Accurate Chemical, Westbury, NY) and incubated for 20 min at room temperature. IgM-opsonized RBCs were further incubated for 20 min at 37°C with C5-deficient human serum (Sigma-Aldrich). Opsonized RBCs were suspended in culture medium and added to macrophages at a 5:1 ratio. After 30 min incubation, cells were fixed in 4% PFA. After several washes in PBS, opsonized RBCs were stained with FITC-conjugated goat anti-rabbit IgG (Invitrogen). Macrophages were labeled with Alexa Fluor 488 phalloidin (Invitrogen). In control experiments, macrophage cultures were incubated for 30 min with FITC-labeled dextran microspheres (Sigma-Aldrich).

The proportion of macrophages containing ingested particles was determined by manually counting >100 macrophages per sample. The phagocytosis index was calculated according to the formula: (number of macrophages containing one ingested particle + number of macrophages containing two ingested particles × 2 + number of macrophages containing three ingested particles × 3 + number of macrophages containing four or more ingested particles × 4) ÷ total number of counted macrophages.

For dynamic imaging, macrophages were cultured in glass-bottom culture dishes (MatTek, Ashland, MA) as described above, and AT uptake was monitored in real time with a Leica AM TIRF microscope in fluorescent widefield-brightfield mode, using a ×40/1.25 oil-immersion objective. Images were acquired with an Andor iXon EMCCD chip.

Gene expression analysis

Peritoneal macrophages were harvested as described previously (18). For ligand assays, macrophages were incubated with 100 nM RSG, 100 nM 9cRA, or 100 nM LG268 (a gift from Reid Bissonette, Ligand Pharmaceuticals, La Jolla, CA) for 24 h. For AT assays, ATs were added to macrophages (5:1) for 30 min or 24 h. When needed, ATs where removed by gentle washing, and macrophages were incubated with 100 ng/ml LPS for an additional 5 h for gene expression analysis or 18 h for cytokine secretion studies. Cytokine secretion was quantified in culture supernatants using commercially available ELISA kits (BD Biosciences). Total macrophage RNA was isolated using Trizol (Sigma-Aldrich). Transcripts were quantified in a two-step RT-quantitative PCR process. First-strand cDNA was synthesized from 1 μg total RNA using the High Capacity cDNA Reverse Transcription Kit (Applied Biosystems, Foster City, CA) with random hexamers. Samples were run in 20 μl reactions using the GeneAmp PCR System 9700 (Applied Biosystems). Quantitative PCR reactions and analyses were then performed using SYBR Green oligonucleotides and the ABI PRISM 7900 FAST Sequence Detection System (Applied Biosystems). The analysis was customized, with two replicates per target gene and two parallel analyses for each biologic sample. Expression levels of target genes were normalized to a standard housekeeping gene (*36b4*) as an internal control. Gene expression values were expressed as relative mRNA level (fold change) compared with untreated controls, based on the standard curve method as described by the manufacturer (Invitrogen). Primer sequences can be provided upon request. Affimetrix U74Av2 microarrays were analyzed as described previously (30). Expression data were visualized using Treeview (Taxonomy and Systematics, Glasgow, U.K.). The microarray data sets have been submitted to the GEO database under accession number GSE24292 (http://www.ncbi.nlm.nih.gov/geo/).

ChIP-seq and peak calling analysis

The generation and analysis of the ChIP-seq data for PPARγ binding and histone H3 lysine 9 acetylation (H3K9Ace) enrichment in mouse macrophages have been described elsewhere (31). Chromatin immunoprecipitations for PPARγ (sc-7196; Santa Cruz Biotechnology) and H3K9Ace (ab4441; Abcam) were performed using primary WT thioglycollate-elicited macrophages, followed by amplification of the precipitated DNA and sequencing of 36-bp reads using the Solexa Analysis Pipeline. The reads were mapped to the mouse genome (mm8) using ELAND. Peak calling for PPARγ was performed using GLITR (32) and the following thresholds were applied to obtain high-confidence binding regions: false discovery rate (FDR) ≤0.5%; fold change over input ≥5; number of reads at the peak summit ≥9. In this study, the FDR threshold was also lowered to 5%, and the additional requirements of fold change and number of reads at the peak summit were eliminated to obtain a less stringent dataset. H3K9Ace data were analyzed using Significance Tester for Accumulation of Reads (http://www.cbil.upenn.edu/STAR) using a threshold of FDR 5%

(33). Areas of input bias, based on peak enrichment in input sequencing runs, were masked in all datasets.

Digital images

Acquisition data are summarized in Supplemental Table 1. Images were acquired with a Nikon BF/Fluo microscope or a Leica AM DIC/TIRF microcope, using an ×40/1.25 oil-immersion objective and an Andor iXon EMCCD chip. We used NIS Elements acquisition software.

Statistical analysis

All data are means ± SEM. Data from histomorphometric analysis, clinical chemistry measurements, and phagocytosis assays were compared by two-tailed paired Student *t* tests. Quantitative PCR data were analyzed by unpaired Student *t* test for comparison of WT and KO samples and by paired Student *t* test for comparison of untreated and treated WT cells. The normal distribution of data were checked by the Kolmogorov-Smirnov test, with $\alpha = 0.05$.

Results

Mice lacking macrophage expression of PPARγ or RXRα develop glomerulonephritis

Conditional KO mice lacking macrophage expression of PPARγ (18) or RXRα (24) were generated by crossing mice bearing the lox-P-targeted PPARγ ($PPAR\gamma^{f/f}$) or RXRα ($RXR\alpha^{f/f}$) alleles with mice bearing the lysozyme-M Cre (LysMCre) recombinase transgene. We refer to LysM Cre-negative $PPAR\gamma^{f/f}$ and $RXR\alpha^{f/f}$ mice as WT, and their $PPAR\gamma^{f/f}LysMCre^{+}$ or $RXR\alpha^{f/f}LysMCre^{+}$ littermates as KO animals (PPARγ-KO and RXRα-KO).

Female mice lacking macrophage expression of PPARγ or RXRα developed severe nephropathy at 4–6 mo old. An early sign of nephritis is enlargement of the renal glomeruli (12), so we analyzed the kidney angioarchitecture by OPT. OPT imaging of renal arteriolar casts revealed enlarged glomeruli in focal regions within the kidneys of PPARγ-KO and RXRα-KO animals (Fig. 1*A*). Kidney hypertrophy, a consequence of glomerulomegaly, caused a significant increase in kidney weight in PPARγ-KO and RXRα-KO mice compared with WT littermates (Supplemental Fig. 1*A*).

Histologic analysis revealed mesangial hypercellularity, mesangial matrix expansion, and basement membrane thickening in PPARγ-KO and RXRα-KO kidneys, and these histopathologic alterations were more evident in older mice (Fig. 1*B*). The increases in glomerular size and glomerular cell number in the KO mice were confirmed by histomorphometric analysis (Fig. 1*C*), and glomerular basement membrane thickening was also visible by silver impregnation (Fig. 1*D*). These histopathologic features of PPARγ-KO and RXRα-KO mice are hallmarks of glomerulonephritis (GN) (34). Moreover, we also detected excretion of albumin (Fig. 1*C*) and high m.w. proteins in the urine of PPARγ-KO and RXRα-KO mice (Supplemental Fig. 1*B*), as well as elevated plasma creatinine levels (Fig. 1*C*), all of which are possible consequences of GN (35, 36).

Transmission electron microscopy (TEM) of nephrons demonstrated that glomerular basement membranes were thickened by 38 ± 6% in PPARγ-KO mice and 35 ± 4% in RXRα-KO mice compared with their WT littermates. TEM also detected coarsening and fusion of podocyte foot processes in PPARγ-KO and RXRα-KO samples (Fig. 1*D*). These findings are consistent with the ultrastructural changes reported in mice with proteinuria (35). Consistently, cell destruction in the glomeruli in PPARγ-KO and RXRα-KO mice was indicated by the accumulation of electro-lucent material in podocyte foot processes (Fig. 1*D*).

Lupus-like anti-DNA Abs accumulate in mice lacking macrophage PPARγ or RXRα

To further characterize the glomerular injury, we examined the localization of inflammatory markers and mouse immunoglobulins by immunohistochemistry. Most glomeruli in the kidneys of PPARγ-KO and RXRα-KO mice contained numerous F4/80-positive inflammatory cells (Fig. 2*A*). These glomeruli also showed strong immunostaining for VEGF-A in the mesangium surrounding the glomerular capillaries, correlating with elevated serum levels of VEGF-A in PPARγ-KO and RXRα-KO mice (Fig. 2*A*, 2*C*). These findings indicate severe glomerular inflammation associated with massive macrophage infiltration (37). In addition, there was a marked deposition of IgG and IgM in the mesangial matrix of PPARγ-KO and RXRα-KO mice (Fig. 2*B*), and analysis of serum showed that these animals developed autoantibodies against nuclear proteins (ANA) (Fig. 2*D*), ssDNA (anti-ssDNA; Fig. 2*E*) and dsDNA (anti-dsDNA; Fig. 2*F*), suggesting an autoimmune origin of the observed GN (1). To determine whether the GN results from changes in lymphoid and myeloid cell subsets, we performed an immunophenotyping analysis of bone marrow, spleen, and lymph nodes in WT, PPARγ-KO, and RXRα-KO mice. The numbers of different leukocyte populations did not differ between WT, PPARγ-KO, and RXRα-KO littermates (Supplemental Fig. 3), suggesting that the expansion of immune cells is not the cause of the observed GN.

Macrophage PPARγ and RXRα are required for normal apoptotic cell clearance

Impaired clearance of apoptotic cells within the kidney glomeruli is thought to contribute to autoimmune GN (12, 38). A significant increase in the number of apoptotic cells in the glomeruli of PPARγ-KO and RXRα-KO mice was detected by TUNEL (Fig. 3*A*, 3*B*). Consistently, PPARγ-KO and RXRα-KO glomeruli were abundant in endothelial and mesangial cells containing cytosolic cleaved caspase-3 (Fig. 3*A*). Immunostaining revealed that cleaved caspase-3 positive apoptotic cells were distributed throughout the spleens of PPARγ-KO and RXRα-KO mice and that a significantly lower proportion of splenic macrophages contained apoptotic cells in these mice (Supplemental Fig. 1*C*), indicating a generalized defect in apoptotic cell clearance (4, 39).

Accumulation of apoptotic cells in the spleen can be caused by insufficient phagocytosis by marginal zone macrophages and can induce the production of autoantibodies against nuclear DNA fragments by marginal zone B cells (12). To investigate whether macrophage phagocytosis was altered in PPARγ-KO or RXRα-KO mice, we injected their peritoneal cavities with fluorescently labeled ATs. Peritoneal lavage showed that ATs were still abundant 6 or 14 h after injection. In contrast, the peritoneal macrophages of similarly

treated WT littermates efficiently scavenged most of the injected ATs (Fig. 3*C*, 3*D*; Supplemental Fig. 2*B*, 2*C*). Phagocytosis deficit of peritoneal macrophages of PPARγ-KO and RXRα-KO mice was also reflected by their notably lower phagosome content and smaller filopodia compared with WT macrophages (Fig. 3*D*). These findings suggest a profound in vivo defect in apoptotic cell clearance in PPARγ-KO and RXRα-KO mice.

PPARγ/RXRα heterodimers regulate the expression of genes involved in the engulfment of apoptotic cells by macrophages

To understand the molecular mechanism underlying the defective apoptotic cell removal detected in our mouse models, we profiled gene expression in WT and knockout macrophages by microarray analysis. Clustering analyses revealed that KO peritoneal macrophages are deficient for the transcription of a set of genes encoding phagocytosis-associated receptors and opsonins (Supplemental Fig. 4*A*). Quantitative PCR analysis confirmed that the expression of *Cd36*, *Axl*, *Mertk*, *Fcgr1*, and the *C1q* subunits *C1qa*, *C1qb*, and *C1qc* was lower in both PPARγ-KO and RXRα-KO macrophages (Fig. 4*A*). In PPARγ-KO macrophages, we also detected a significant downregulation of genes encoding other phagocytosis related molecules, including *Tgm2*, *Mfge8*, *Lrp1*, *Itgam*, *Itgax*, and *C3* (Fig. 4*A*; Supplemental Fig. 4*B*). In contrast, PPARγ and RXRα deficiency had no effect on the expression of the macrophage receptors *Cd14*, *Calr*, and *Itga5* or the opsonins *Gas6* and *Thbs1* (Supplemental Fig. 4*B*).

The digestion of apoptotic cells by macrophages leads to the accumulation of cellular components, including cholesterol and fatty acids, that could act as endogenous ligands of PPARγ and RXRα (16). To investigate this possibility, we analyzed the expression of phagocytosis-related genes in WT, PPARγ-KO, and RXRα-KO peritoneal macrophages incubated with ATs. The presence of ATs increased the expression of *Cd36*, *Mertk*, *Axl*, *Fcgr1*, *C1qa*, *C1qb*, *C1qc*, and *Tgm2* in WT macrophages, but not in PPARγ-KO and RXRα-KO macrophages (Fig. 4*B*). Apoptotic cell components thus enhance the expression of macrophage receptors and opsonins required for further apoptotic cell uptake, via a PPARγ- and RXRα-dependent mechanism.

We next tested whether the expression of these genes can be modulated by pharmacologic activation of PPARγ or RXRα. Peritoneal macrophages from WT, PPARγ-KO, and RXRα-KO mice were cultured for 24 h in the presence of PPARγ or RXRα agonists (RSG for PPARγ, 9cRA and LG268 for RXRα). All three agonists selectively induced the expression of *Cd36*, *Mertk*, *Axl*, *Fcgr1*, and *Tgm2* in WT macrophages but not in PPARγ-KO or RXRα-KO cells (Fig. 4*C*; Supplemental Fig. 5*A*). Furthermore, the expression levels of *C1qa*, *C1qb*, and *C1qc* were also upregulated in WT macrophages treated with RXRα ligands (Fig. 4*C*; Supplemental Fig. 5*A*). None of these *C1q* isoforms was regulated by RSG, although RSG strongly upregulated the expression of the PPARγ target genes ATP-binding cassette transporter G1 *(Abcg1)* and adipose differentiation-related protein (*Adrp*) in WT macrophages (Supplemental Fig. 4*E*). PPARγ or RXRα agonists did not significantly induce the expression in WT macrophages of the receptors *Cd14*, *Calr*, *Itga5*, *Lrp1*, *It gam*, and *Itgax* and the opsonins *Gas6*, *Thbs1*, *C3*, and *Mfge8* (Supplemental Fig. 4*C*, 4*D*).

In PPARγ-KO macrophages, but not in RXRα-KO cells, the RXRα ligand LG268 moderately elevated the transcription of *Cd36*, *Mertk*, *Axl*, *Fcgr1*, *Tgm2*, and the *C1q* isoforms, reflecting the ability of RXRα to form heterodimers with other partners. In contrast, in RXRα-KO macrophages the action of the PPARγ agonist RSG was severely impaired, with only a mild increase in *Cd36* expression detected that was significantly below that seen in WT cells (Supplemental Fig. 5*B*).

Further confirmation that the phagocytosis genes *Cd36*, *Mertk*, *Axl*, *Fcgr1*, and *Tgm2* are directly regulated by PPARγ was obtained by assessing genomic PPARγ binding in peritoneal macrophages (31) by chromatin immunoprecipitation followed by high-throughput sequencing (ChIP-seq). In this analysis, *Cd36*, *Axl*, *Fcgr1*, and *Tgm2* all had high-confidence PPARγ binding regions within 100 kb of their transcription start sites, using an FDR of 0.5% (Fig. 4*D*, blue track). Relaxing the threshold to an FDR of 5% revealed that additional binding regions near these genes and also near *Mertk* (Fig. 4*D*, red track). Importantly, many of these PPARγ binding regions were found to overlap with statistically significant regions of H3K9Ace (Fig. 4*D*, black track), a chromatin mark often found at enhancers and promoters of active genes (40, 41). Considering the responsiveness to a PPARγ ligand and reduced expression in PPARγ- and RXRα-deficient macrophages, the data strongly suggest that these genes are likely to be under the direct transcriptional control of PPARγ/RXRα.

Diminished anti-inflammatory response to apoptotic cells in macrophages lacking PPARγ or RXRα

Phagocytosis of apoptotic cells by macrophages promotes their differentiation to a regulatory or deactivated phenotype that is closely associated with the diminished production of inflammatory mediators and the induction of self-tolerance (5, 7–9). These macrophages are characterized by the production of the anti-inflammatory cytokines TGF-β and IL-10 and the expression of surface markers as the mannose receptor and the signaling lymphocytic activation molecule (8, 42). We found that engulfment of ATs upregulates the anti-inflammatory cytokine genes *Tgfb1* and *Il10* and the cellsurface marker genes *Mrc1* (encoding mannose receptor) and *Slam* (encoding signaling lymphocytic activation molecule) in WT macrophages. These genes were not affected or were affected to a lesser extent in PPARγ-KO and RXRα-KO macrophages (Fig. 5*A*). Accordingly, in PPARγ-KO and RXRα-KO mice, splenic macrophages showed a strongly reduced immunostaining for IL-10 (Supplemental Fig. 1*D*).

To test the possible involvement of PPARγ and RXRα in the regulation of proinflammatory cytokine production, we analyzed inflammatory gene expression in WT, PPARγ-KO, and RXRα-KO macrophages stimulated with LPS in the presence or absence of ATs (Fig. 5*B*). LPS upregulated the expression of genes encoding IL-12B (*Il12b*), IL-1β (*Il1b*), iNOS (*Nos2*, *iNOS*), and TNF-α (*Tnf*). The presence of ATs significantly reduced the transcript levels of these proinflammatory markers in WT macrophages, but had no effect on PPARγ-KO and RXRα-KO macrophages (Fig. 5*B*). Cytokine secretion was also monitored by ELISA. As expected, the presence of ATs suppressed the release of proinflammatory

cytokines by WT macrophages, but had little effect on PPARγ-KO and RXRα-KO macrophages (Supplemental Fig. 6).

Consistently, the kidney glomeruli of PPARγ-KO and RXRα-KO mice were infiltrated with cells expressing proinflammatory markers, such as IL-1β, iNOS, and TNF-α (Fig. 5*C*). These data indicate that the observed GN in mice lacking macrophage expression of PPARγ or RXRα might be a consequence of impaired apoptotic cell removal and enhanced proinflammatory macrophage activation within the kidney glomeruli.

Apoptotic cell uptake is impaired in macrophages lacking PPARγ or RXRα

To determine directly whether macrophages from PPARγ-KO and RXRα-KO mice were defective in apoptotic cell uptake we tested the ability of peritoneal macrophages to ingest fluorescently-labeled ATs in vitro. Compared with WT cells, PPARγ-KO and RXRα-KO peritoneal macrophages were markedly deficient in the phagocytosis of fluorescently labeled ATs (Fig. 6*A*, B), with a significantly lower average number of ATs scavenged per macrophage (phagocytosis index; Fig. 6*C*, 6*D*). This defect was also reflected in a reduced percentage of macrophages containing ingested ATs (Supplemental Fig. 7*A*, 7*B*). Phagocytosis of ATs by WT macrophages was significantly enhanced by pharmacologic activation of PPARγ or RXRα, increasing both the phagocytosis index (Fig. 6*AD*) and the percentage of WT cells containing ATs (Supplemental Fig. 7*A*, 7*B*). Treatment of PPARγ-KO or RXRα-KO macrophages with RSG or 9cRA had no effect on either parameter (Fig. 6*C*, 6*D*; Supplemental Fig. 7*A*, 7*B*). Real-time microscopy recordings indicated that PPARγ-KO and RXRα-KO macrophages were deficient in AT binding (Fig. 6*E*, 6*F*), and treatment with RSG or 9cRA strongly increased the AT binding ability of WT macrophages, but had no effect on macrophages lacking PPARγ or RXRα (Fig. 6*G*, 6*H*). Altered *Fcgr1* and *C1q* expression was reflected by an impaired phagocytosis of Ig-opsonized (IgG and IgM, respectively) particles by PPARγ-KO and RXRα-KO macrophages (Supplemental Figs. 7*D–G*, 8). In contrast, macrophage deficiency in PPARγ or RXRα had no effect on the uptake of fluorescent beads (Supplemental Fig. 7*C*).

Discussion

Our findings indicate that macrophage PPARγ and RXRα are required for the efficient disposal of apoptotic bodies, which prevents the release of intracellular components and the consequent loss of immunological self-tolerance, and might explain the development of an SLE-like nephritis in mice lacking macrophage PPARγ or RXRα. Indeed, altered PPARγ function has been linked to other autoimmune diseases, such as multiple sclerosis in humans and autoimmune encephalomyelitis in mouse (43). Our results show that the mechanism underlying the phagocytosis deficit of PPARγ-KO and RXRα-KO macrophages involves the disruption of a network of genes regulated by PPARγ/RXRα heterodimers. This gene network includes the cell surface receptors *Cd36*, *Mertk*, *Axl*, and *Fcgr1*, all of which are required for the proper binding and consequent internalization of apoptotic cells (9); *Tgm2*, which encodes a protein involved in apoptotic cell uptake (44); and the opsonins *C1qa*, *C1qb* and *C1qc*, which bind to the apoptotic cell surface to initiate phagocytosis (45). This coordinated regulation of phagocytosis-related genes indicates an important role for PPARγ/

RXRα heterodimers in the clearance of apoptotic cells. However, the ability of the RXRα ligand LG268 to induce limited expression of these genes in PPARγ-KO macrophages suggests that they can be also regulated by other heterodimer partners of RXRα. Consistenly, two of these genes, *Mertk* and *C1qb*, have been shown to be targets of liver X receptor or PPARδ (39, 46). These findings indicate that RXRα can modulate the expression of phagocytosis-related genes by forming heterodimers with different partners.

There are considerable data supporting the idea that deficits in the expression of macrophage receptors and opsonins can lead to deficient apoptotic cell clearance and autoimmunity (11, 38, 39, 47). However, some mouse models of defective apoptotic cell removal do not have autoimmune disease (7, 48), suggesting that additional mechanisms contribute to the development of self immunity. The lack of the opsonin C1q in mice leads to altered apoptotic cell uptake and autoimmune disease with glomerular inflammation, which is similar to our present findings (13). Moreover, homozygous deficiency for C1q is associated with increased susceptibility to SLE in humans (13). There is also evidence that lack of MERTK and AXL results in widespread accumulation of apoptotic cells and autoantibody production in mice (49). Loss of MERTK alters macrophage cytokine production and impairs phagocytosis of apoptotic cells, leading to the development of a progressive SLE-like autoimmunity (50). Therefore, the lack of expression of these macrophage receptors and opsonins provides a possible molecular explanation for the deficient engulfment of apoptotic cells and the development of GN in PPARγ-KO and RXRα-KO mice.

Macrophages phagocytosing apoptotic cells accumulate cellular components, including cholesterol and fatty acids, that are potential activators of PPARγ/RXRα (51). Our results suggest that the activation of PPARγ/RXRα in this context has distinct effects on phagocytosis and the preservation of self-tolerance. First, PPARγ/RXRα activates the transcription of genes involved in phagocytosis, thereby mediating the rapid and early removal of dying cells and avoiding accumulation of their harmful intracellular components. Second, the PPARγ/RXRα mediated safe removal of apoptotic cells, which provokes a shift to a so-called regulatory or deactivated anti-inflammatory macrophage phenotype characterized by enhanced *Tgfb1*, *Il10*, *Slam*, and *Mrc1* gene expression (8, 42) as well as reduction of proinflammatory genes such as *Il1b*, *Il12b*, *Il6*, *Nos2* and *Tnf*. The inhibition of proinflammatory genes may be due to a direct transrepression activity of PPARγ by the ligand-dependent antagonism of the NF-κB (15). Apoptotic cells have been shown to induce PPARγ sumoylation, which is targeted to the nuclear receptor corepressor, blocking its clearance from NF-κB sites within proinflammatory promoters (52). In addition, the PPARγ/RXRα-mediated induction of *Mertk* and *Axl* may negatively regulate inflammatory mediators by controlling the expression of the suppressor of cytokine signaling proteins SOCS1 and SOCS3 (50).

Approaches aimed at resolving the core autoimmune disorder in SLE are at various stages of preclinical and clinical development, and they include immunosuppressive therapy and eventually hematopoietic stem cell transplantation (1). Ligands for PPARγ, such as RSG and pioglitazone (thiazolidinediones) can reduce renal inflammation and macrophage infiltration of kidney cortex in murine models of SLE (53), mainly through the modulation of mesangial cell functions (53, 54). Activation of PPARγ has also been proposed to

ameliorate SLE nephritis through the upregulation of the synthesis of the anti-inflammatory factor adiponectin in adipocytes (55). Thiazolidinediones are already in clinical use as insulin sensitizers with antiatherogenic effects (56). This represents an advantage in regard to other nuclear receptors such as PPARδ and liver X receptor, whose ligands have not been introduced to clinical practice. Moreover, the overlapping effects of PPARγ and RXRα ligands on phagocytosis raise the possibility that dual administration of PPARγ and RXRα activators could allow the administration of lower doses of thiazolidinediones, reducing their side effects (56). Our work suggests a new therapeutic potential for PPARγ/RXRα ligands as enhancers of apoptotic cell removal by macrophages. Therefore, we anticipate that our findings will be a starting point for studies aimed at the selective modulation of macrophage PPARγ/RXRα potential targets for the treatment of SLE.

Supplementary Material

Refer to Web version on PubMed Central for supplementary material.

Acknowledgments

This work was supported by grants from the Spanish Ministry of Science and Innovation (SAF2009-07466), the Fundación Genoma España, and Marató TV3 (to M.R.), and by grants from the Fundación Genoma España and the Spanish Ministry of Health (FIS PI052270) (to T.F.). T.R. is supported by the People Marie Curie Intra-European Fellowships Program. M.R. and T.F. are supported by the Ramón y Cajal Program. Centro Nacional de Investigaciones Cardiovasculares is supported by the Spanish Ministry of Science and Innovation and the Pro-CNIC Foundation.

We thank Dr. Christian Hellriegel and Dr. Rubén Mota (Centro Nacional de Investigaciones Cardiovasculares [CNIC]), Roisin Brid Doohan (Histopathology Unit, CNIC), and Francisco Urbano Olmos and Covadonga Aguado Ballano (Transmission Electron Microscopy Laboratory, Universidad Autónoma, Madrid, Spain) for help and advice. We also thank Simon Bartlett for editorial assistance. The optical microscopy work described in this study was conducted at the Microscopy and Dynamic Imaging Unit, CNIC, Madrid, Spain.

Abbreviations used in this paper

ANA	anti-nuclear Ab
AT	apoptotic thymocyte
bm	basement membrane
CNIC	Centro Nacional de Investigaciones Cardiovasculares
9cRA	9-*cis*-retinoic acid
FDR	false discovery rate
GN	glomerulonephritis
H3K9Ace	histone H3 lysine 9 acetylation
iNOS	inducible NO synthase
KO	knockout
OPT	optical projection tomography
PAS	periodic acid-Schiff

pdc	podocyte
PFA	paraformaldehyde
PPARγ	peroxisome proliferator-activated receptor γ
PrI	propidium iodide staining of nuclei
RSG	rosiglitazone
RXR	retinoid X receptor
SLE	systemic lupus erythematosus
TEM	transmission electron microscopy
VEGF-A	vascular endothelial growth factor A
WT	wild type

References

1. Ermann J, Bermas BL. The biology behind the new therapies for SLE. Int J Clin Pract. 2007; 61:2113–2119. [PubMed: 17997810]
2. Kaplan MJ. Management of cardiovascular disease risk in chronic inflammatory disorders. Nat Rev Rheumatol. 2009; 5:208–217. [PubMed: 19337285]
3. Herrmann M, Voll RE, Zoller OM, Hagenhofer M, Ponner BB, Kalden JR. Impaired phagocytosis of apoptotic cell material by monocyte-derived macrophages from patients with systemic lupus erythematosus. Arthritis Rheum. 1998; 41:1241–1250. [PubMed: 9663482]
4. Ravichandran KS, Lorenz U. Engulfment of apoptotic cells: signals for a good meal. Nat Rev Immunol. 2007; 7:964–974. [PubMed: 18037898]
5. Paidassi H, Tacnet-Delorme P, Arlaud GJ, Frachet P. How phagocytes track down and respond to apoptotic cells. Crit Rev Immunol. 2009; 29:111–130. [PubMed: 19496743]
6. Erwig LP, Henson PM. Clearance of apoptotic cells by phagocytes. Cell Death Differ. 2008; 15:243–250. [PubMed: 17571081]
7. Erwig LP, Henson PM. Immunological consequences of apoptotic cell phagocytosis. Am J Pathol. 2007; 171:2–8. [PubMed: 17591947]
8. Mosser DM, Edwards JP. Exploring the full spectrum of macrophage activation. Nat Rev Immunol. 2008; 8:958–969. [PubMed: 19029990]
9. Weigert A, Jennewein C, Brüne B. The liaison between apoptotic cells and macrophages—the end programs the beginning. Biol Chem. 2009; 390:379–390. [PubMed: 19335180]
10. Chung EY, Kim SJ, Ma XJ. Regulation of cytokine production during phagocytosis of apoptotic cells. Cell Res. 2006; 16:154–161. [PubMed: 16474428]
11. Cohen PL, Caricchio R, Abraham V, Camenisch TD, Jennette JC, Roubey RA, Earp HS, Matsushima G, Reap EA. Delayed apoptotic cell clearance and lupus-like autoimmunity in mice lacking the c-mer membrane tyrosine kinase. J Exp Med. 2002; 196:135–140. [PubMed: 12093878]
12. Hanayama R, Tanaka M, Miyasaka K, Aozasa K, Koike M, Uchiyama Y, Nagata S. Autoimmune disease and impaired uptake of apoptotic cells in MFG-E8-deficient mice. Science. 2004; 304:1147–1150. [PubMed: 15155946]
13. Truedsson L, Bengtsson AA, Sturfelt G. Complement deficiencies and systemic lupus erythematosus. Autoimmunity. 2007; 40:560–566. [PubMed: 18075790]
14. Bensinger SJ, Tontonoz P. Integration of metabolism and inflammation by lipid-activated nuclear receptors. Nature. 2008; 454:470–477. [PubMed: 18650918]

15. Ricote M, Glass CK. PPARs and molecular mechanisms of transrepression. Biochim Biophys Acta. 2007; 1771:926–935. [PubMed: 17433773]

16. Kliewer SA, Xu HE, Lambert MH, Willson TM. Peroxisome proliferator-activated receptors: from genes to physiology. Recent Prog Horm Res. 2001; 56:239–263. [PubMed: 11237216]

17. Tontonoz P, Nagy L, Alvarez JG, Thomazy VA, Evans RM. PPARgamma promotes monocyte/macrophage differentiation and uptake of oxidized LDL. Cell. 1998; 93:241–252. [PubMed: 9568716]

18. Hevener AL, Olefsky JM, Reichart D, Nguyen MT, Bandyopadyhay G, Leung HY, Watt MJ, Benner C, Febbraio MA, Nguyen AK, et al. Macrophage PPAR gamma is required for normal skeletal muscle and hepatic insulin sensitivity and full antidiabetic effects of thiazolidinediones. J Clin Invest. 2007; 117:1658–1669. [PubMed: 17525798]

19. Metzger D, Chambon P. Contribution of targeted conditional somatic mutagenesis to deciphering retinoid X receptor functions and to generating mouse models of human diseases. Handb Exp Pharmacol. 2007; 178:511–524. [PubMed: 17203669]

20. Ricote M, Snyder CS, Leung HY, Chen J, Chien KR, Glass CK. Normal hematopoiesis after conditional targeting of RXRalpha in murine hematopoietic stem/progenitor cells. J Leukoc Biol. 2006; 80:850–861. [PubMed: 16888087]

21. Boehm MF, Zhang L, Zhi L, McClurg MR, Berger E, Wagoner M, Mais DE, Suto CM, Davies JA, Heyman RA, et al. Design and synthesis of potent retinoid X receptor selective ligands that induce apoptosis in leukemia cells. J Med Chem. 1995; 38:3146–3155. [PubMed: 7636877]

22. Argmann CA, Sawyez CG, McNeil CJ, Hegele RA, Huff MW. Activation of peroxisome proliferator-activated receptor gamma and retinoid X receptor results in net depletion of cellular cholesteryl esters in macrophages exposed to oxidized lipoproteins. Arterioscler Thromb Vasc Biol. 2003; 23:475–482. [PubMed: 12615696]

23. Reddy RC. Immunomodulatory role of PPAR-gamma in alveolar macrophages. J Investig Med. 2008; 56:522–527.

24. Núñez V, Alameda D, Rico D, Mota R, Gonzalo P, Cedenilla M, Fischer T, Boscá L, Glass CK, Arroyo AG, Ricote M. Retinoid X receptor alpha controls innate inflammatory responses through the up-regulation of chemokine expression. Proc Natl Acad Sci USA. 2010; 107:10626–10631. [PubMed: 20498053]

25. Sharpe J, Ahlgren U, Perry P, Hill B, Ross A, Hecksher-Sørensen J, Baldock R, Davidson D. Optical projection tomography as a tool for 3D microscopy and gene expression studies. Science. 2002; 296:541–545. [PubMed: 11964482]

26. Sharma K, McCue P, Dunn SR. Diabetic kidney disease in the db/db mouse. Am J Physiol Renal Physiol. 2003; 284:F1138–F1144. [PubMed: 12736165]

27. Yumura W, Sugino N, Nagasawa R, Kubo S, Hirokawa K, Maruyama N. Age-associated changes in renal glomeruli of mice. Exp Gerontol. 1989; 24:237–249. [PubMed: 2731581]

28. Scott RS, McMahon EJ, Pop SM, Reap EA, Caricchio R, Cohen PL, Earp HS, Matsushima GK. Phagocytosis and clearance of apoptotic cells is mediated by MER. Nature. 2001; 411:207–211. [PubMed: 11346799]

29. Djaldetti M, Salman H, Bergman M, Straussberg R, Alexandrova S, Bessler H. A simple method for evaluation of latex phagocytosis by rat peritoneal macrophages. Acta Haematol. 1997; 98:56–57. [PubMed: 9210918]

30. Welch JS, Ricote M, Akiyama TE, Gonzalez FJ, Glass CK. PPARgamma and PPARdelta negatively regulate specific subsets of lipopolysaccharide and IFN-gamma target genes in macrophages. Proc Natl Acad Sci USA. 2003; 100:6712–6717. [PubMed: 12740443]

31. Lefterova MI, Steger DJ, Zhuo D, Qatanani M, Mullican SE, Tuteja G, Manduchi E, Grant GR, Lazar MA. Cell-specific determinants of peroxisome proliferator-activated receptor gamma function in adipocytes and macrophages. Mol Cell Biol. 2010; 30:2078–2089. [PubMed: 20176806]

32. Tuteja G, White P, Schug J, Kaestner KH. Extracting transcription factor targets from ChIP-Seq data. Nucleic Acids Res. 2009; 37:e113. [PubMed: 19553195]

33. Steger DJ, Grant GR, Schupp M, Tomaru T, Lefterova MI, Schug J, Manduchi E, Stoeckert CJ Jr, Lazar MA. Propagation of adipogenic signals through an epigenomic transition state. Genes Dev. 2010; 24:1035–1044. [PubMed: 20478996]
34. Huber TB, Kwoh C, Wu H, Asanuma K, Gödel M, Hartleben B, Blumer KJ, Miner JH, Mundel P, Shaw AS. Bigenic mouse models of focal segmental glomerulosclerosis involving pairwise interaction of CD2AP, Fyn, and synaptopodin. J Clin Invest. 2006; 116:1337–1345. [PubMed: 16628251]
35. Mundel P, Shankland SJ. Podocyte biology and response to injury. J Am Soc Nephrol. 2002; 13:3005–3015. [PubMed: 12444221]
36. Ritz E. Renal dysfunction as a novel risk factor: microalbuminuria and cardiovascular risk. Kidney Int Suppl. 2005; 67:S25–S28. [PubMed: 15613063]
37. Foster RR. The importance of cellular VEGF bioactivity in the development of glomerular disease. Nephron, Exp Nephrol. 2009; 113:e8–e15. [PubMed: 19590237]
38. Davidson A, Aranow C. Lupus nephritis: lessons from murine models. Nat Rev Rheumatol. 2010; 6:13–20. [PubMed: 19949431]
39. A-Gonzalez N, Bensinger SJ, Hong C, Beceiro S, Bradley MN, Zelcer N, Deniz J, Ramirez C, Díaz M, Gallardo G, et al. Apoptotic cells promote their own clearance and immune tolerance through activation of the nuclear receptor LXR. Immunity. 2009; 31:245–258. [PubMed: 19646905]
40. Heintzman ND, Stuart RK, Hon G, Fu Y, Ching CW, Hawkins RD, Barrera LO, Van Calcar S, Qu C, Ching KA, et al. Distinct and predictive chromatin signatures of transcriptional promoters and enhancers in the human genome. Nat Genet. 2007; 39:311–318. [PubMed: 17277777]
41. Heintzman ND, Hon GC, Hawkins RD, Kheradpour P, Stark A, Harp LF, Ye Z, Lee LK, Stuart RK, Ching CW, et al. Histone modifications at human enhancers reflect global cell-type-specific gene expression. Nature. 2009; 459:108–112. [PubMed: 19295514]
42. Mantovani A, Sica A, Sozzani S, Allavena P, Vecchi A, Locati M. The chemokine system in diverse forms of macrophage activation and polarization. Trends Immunol. 2004; 25:677–686. [PubMed: 15530839]
43. Klotz L, Schmidt S, Heun R, Klockgether T, Kölsch H. Association of the PPARgamma gene polymorphism Pro12Ala with delayed onset of multiple sclerosis. Neurosci Lett. 2009; 449:81–83. [PubMed: 18977277]
44. Tóth B, Garabuczi E, Sarang Z, Vereb G, Vámosi G, Aeschlimann D, Blaskó B, Bécsi B, Erdõdi F, Lacy-Hulbert A, et al. Transglutaminase 2 is needed for the formation of an efficient phagocyte portal in macrophages engulfing apoptotic cells. J Immunol. 2009; 182:2084–2092. [PubMed: 19201861]
45. Hart SP, Smith JR, Dransfield I. Phagocytosis of opsonized apoptotic cells: roles for ‘old-fashioned’ receptors for antibody and complement. Clin Exp Immunol. 2004; 135:181–185. [PubMed: 14738443]
46. Mukundan L, Odegaard JI, Morel CR, Heredia JE, Mwangi JW, Ricardo-Gonzalez RR, Goh YP, Eagle AR, Dunn SE, Awakuni JU, et al. PPAR-delta senses and orchestrates clearance of apoptotic cells to promote tolerance. Nat Med. 2009; 15:1266–1272. [PubMed: 19838202]
47. Botto M. Links between complement deficiency and apoptosis. Arthritis Res. 2001; 3:207–210. [PubMed: 11438036]
48. Cacciapaglia F, Spadaccio C, Chello M, Gigante A, Coccia R, Afeltra A, Amoroso A. Apoptotic molecular mechanisms implicated in autoimmune diseases. Eur Rev Med Pharmacol Sci. 2009; 13:23–40. [PubMed: 19364083]
49. Seitz HM, Camenisch TD, Lemke G, Earp HS, Matsushima GK. Macrophages and dendritic cells use different Axl/Mertk/Tyro3 receptors in clearance of apoptotic cells. J Immunol. 2007; 178:5635–5642. [PubMed: 17442946]
50. Lemke G, Rothlin CV. Immunobiology of the TAM receptors. Nat Rev Immunol. 2008; 8:327–336. [PubMed: 18421305]
51. Henson P. Suppression of macrophage inflammatory responses by PPARs. Proc Natl Acad Sci USA. 2003; 100:6295–6296. [PubMed: 12756292]

52. Jennewein C, Kuhn AM, Schmidt MV, Meilladec-Jullig V, von Knethen A, Gonzalez FJ, Brüne B. Sumoylation of peroxisome proliferator-activated receptor gamma by apoptotic cells prevents lipopolysaccharide-induced NCoR removal from kappaB binding sites mediating transrepression of proinflammatory cytokines. J Immunol. 2008; 181:5646–5652. [PubMed: 18832723]

53. Venegas-Pont M, Sartori-Valinotti JC, Maric C, Racusen LC, Glover PH, McLemore GR Jr, Jones AV, Reckelhoff JF, Ryan MJ. Rosiglitazone decreases blood pressure and renal injury in a female mouse model of systemic lupus erythematosus. Am J Physiol Regul Integr Comp Physiol. 2009; 296:R1282–R1289. [PubMed: 19193937]

54. Kawai T, Masaki T, Doi S, Arakawa T, Yokoyama Y, Doi T, Kohno N, Yorioka N. PPAR-gamma agonist attenuates renal interstitial fibrosis and inflammation through reduction of TGF-beta. Lab Invest. 2009; 89:47–58. [PubMed: 19002105]

55. Aprahamian T, Bonegio RG, Richez C, Yasuda K, Chiang LK, Sato K, Walsh K, Rifkin IR. The peroxisome proliferator-activated receptor gamma agonist rosiglitazone ameliorates murine lupus by induction of adiponectin. J Immunol. 2009; 182:340–346. [PubMed: 19109165]

56. Elte JW, Blicklé JF. Thiazolidinediones for the treatment of type 2 diabetes. Eur J Intern Med. 2007; 18:18–25. [PubMed: 17223037]

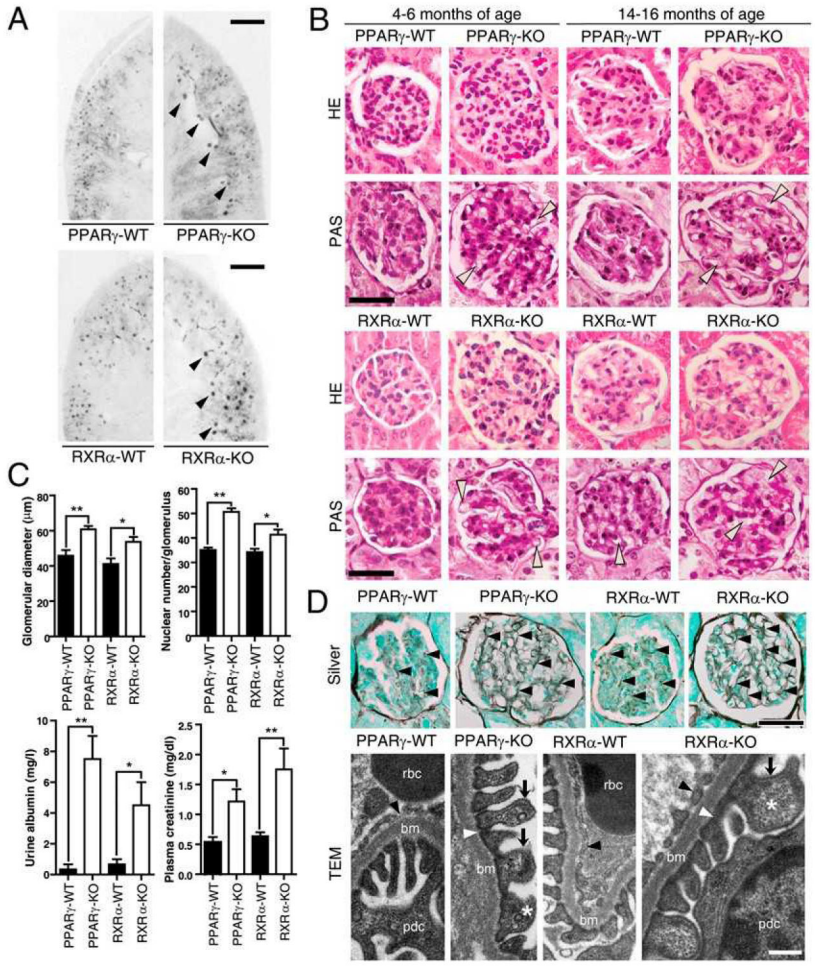

FIGURE 1.

Glomerular inflammation in PPARγ-KO and RXRα-KO mice. *A*, Glomerular angioarchitecture was analyzed by OPT. Arrowheads indicate enlarged glomeruli. Scale bar, 2 mm. *B*, H&E- and PAS-stained sections of the renal cortex. Arrowheads show thickened capillary walls. Scale bar, 30 μm. *C*, Histomorphometric analysis was performed on kidney sections of 4–6-mo-old WT, PPARγ-KO, and RXRα-KO mice. Data are means ± SEM from six mice per genotype. Plasma creatinine levels and albumin content in pooled urine collected over 24 h are expressed as mean values ± SEM from four mice per genotype. *$p < 0.05$; **$p < 0.01$. *D*, *Top*, Silver impregnation of kidney sections from 4–6-mo-old mice. Arrowheads indicate basement membranes. Scale bar, 20 μm. *Bottom*, Transmission electron microscopy (TEM) analysis of the glomerular walls in 4–6-mo-old mice. Thickening (arrows) and fusions (white arrowheads) of the podocyte (pdc) foot processes are visible in PPARγ-KO and RXRα-KO mice. Accumulation of electrolucent material in podocyte processes (asterisks) and a moderate thickening of glomerular basement membrane (bm) are also evident. Black arrowheads label endothelial cells. Scale bar, 0.1 μm.

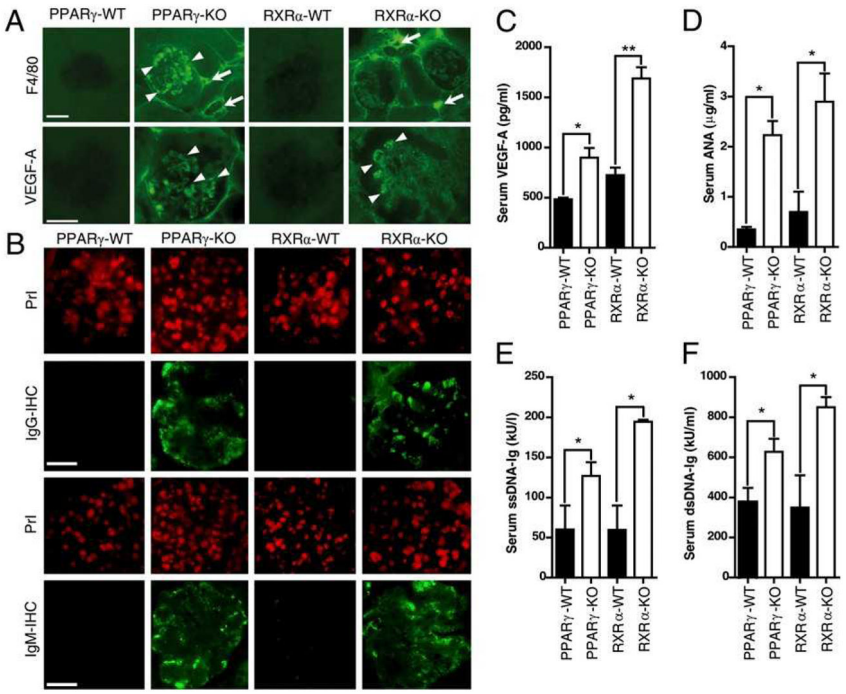

FIGURE 2.

Macrophage-specific PPARγ-KO and RXRα-KO mice show increased renal macrophage infiltration and autoanti-body production. *A*, Immunohistochemical labeling of F4/80 positive cells and VEGF-A deposition in glomeruli of 4–6-mo-old mice. Scale bar, 20 μm. *B*, Immunostaining of IgG (IgG-IHC) and IgM (IgM-IHC) in the glomerular mesangium. PrI, propidium iodide staining of nuclei; scale bar, 20 μm. *C–F*, Serum titers of VEGF-A and auto-antibodies to nuclear proteins (ANA) and to ssDNA and dsDNA (ssDNA-Ig, dsDNA-Ig) are expressed as means ± SEM from six mice per genotype, aged 4–6 mo. *$p < 0.05$; **$p < 0.01$.

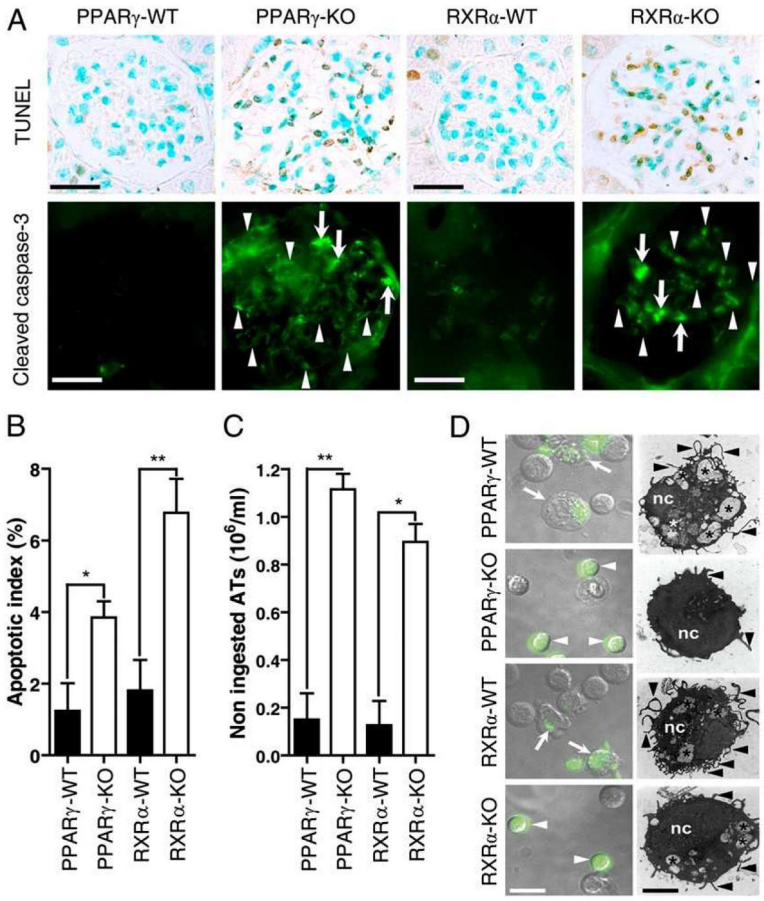

FIGURE 3.

Clearance of apoptotic cells in vivo is impaired in PPARγ-KO and RXRα-KO mice. *A*, Abundance of TUNEL-positive (brown nuclear staining) and cleaved caspase-3 positive cells (arrowheads indicate endothelial cells; arrows indicate mesangial cells and podocytes) in the glomeruli of 4–6-mo-old PPARγ-KO and RXRα-KO mice. Scale bar, 20 μm. *B*, Apoptotic index, determined by counting TUNEL-positive nuclei in >50 glomeruli of five mice per genotype; the glomeruli of PPARγ-KO and RXRα-KO animals contain elevated numbers of apoptotic cells. Data are means ± SEM. *C*, Four mice per genotype were injected i.p. with fluorescently-labeled ATs, and peritoneal lavage was examined 14 h later. Data are means ± SEM; $*p < 0.05$; $**p < 0.01$. *D*, *Left*, In WT mice, peritoneal macrophages ingested most ATs (white arrows), whereas noningested ATs were abundant (white arrowheads) in PPARγ-KO and RXRα-KO mice. Scale bar, 15 μm. *Right*, TEM images of peritoneal macrophages revealing less phagosomes (asterisks), smaller filopodia, and cell-surface extrusions (black arrowheads) in PPARγ-KO and RXRα-KO cells. Scale bar, 6 μm.

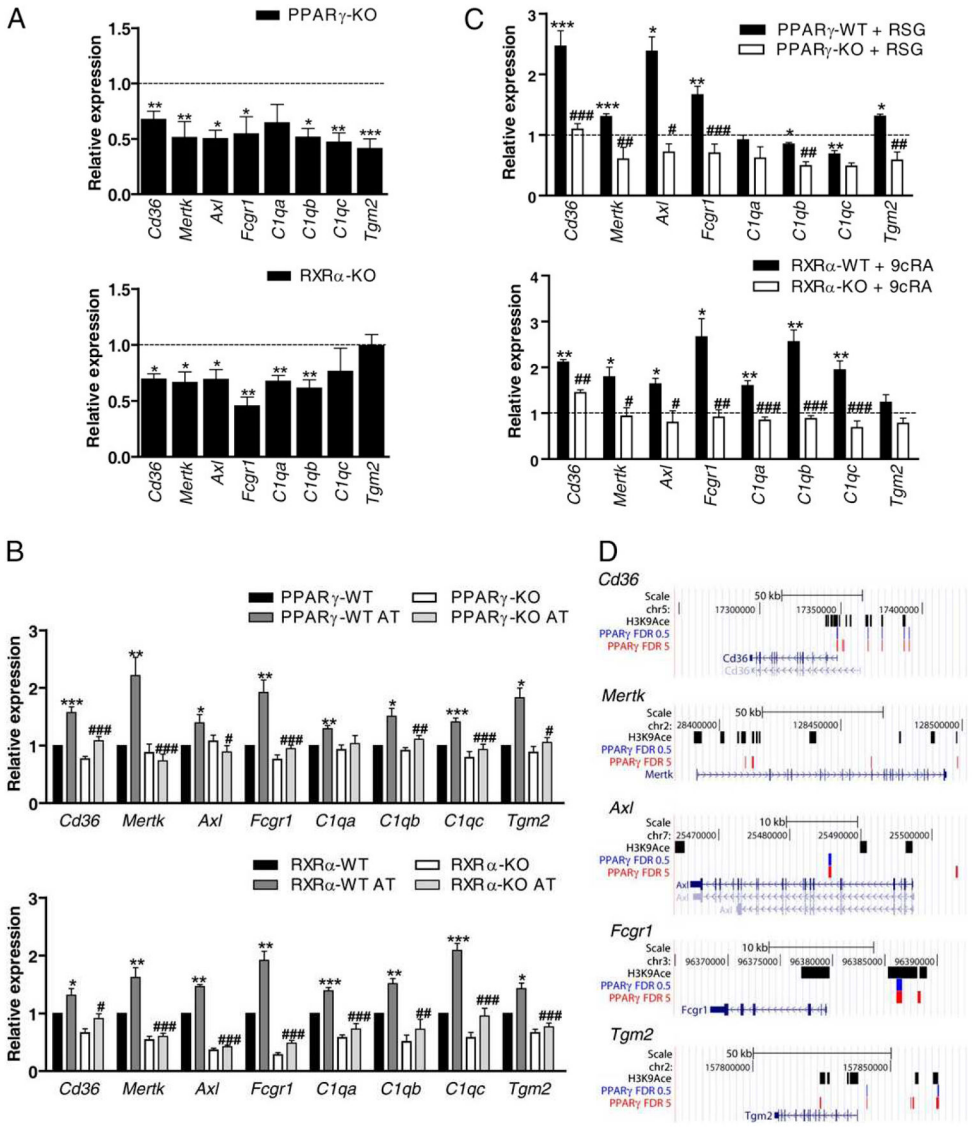

FIGURE 4.

PPARγ/RXRα heterodimers regulate the expression of macrophage receptors and opsonins involved in the engulfment of apoptotic cells. *A*, mRNA expression of engulfment-related genes evaluated by real-time PCR in macrophages derived from six WT, PPARγ-KO, and RXRα-KO mice. The expression of each gene is represented as the fold induction in KO macrophages compared with WT (dashed line). *$p < 0.05$; **$p < 0.01$; ***$p < 0.001$. *B*, mRNA expression of peritoneal macrophages treated with vehicle (PPARγ-WT, PPARγ-KO, RXRα-WT, and RXRα-KO) or ATs (PPARγ-WT AT, PPARγ-KO AT, RXRα-WT AT, and RXRα-KO AT) at 5:1 AT/macrophage ratio for 24 h. Gene expression is represented as fold induction compared with vehicle treated WT cells. *$p < 0.05$, **$p < 0.01$, and ***$p < 0.001$ versus RXRα-WT or PPARγ-WT; $^{\#}p < 0.05$, $^{\#\#}p < 0.01$, and $^{\#\#\#}p < 0.001$ versus RXRα-WT or PPARγ-WT treated with ATs. *C*, Peritoneal macrophages from WT and PPARγ-KO or RXRα-KO mice were treated for 24 h with 100 nM RSG or 100 nM 9cRA. The expression of each gene was measured by real-time PCR and is presented

relative to the expression of each gene in vehicle (ethanol)-treated WT macrophages (dashed line). *$p < 0.05$, **$p < 0.01$, and ***$p < 0.001$ versus RXRα-WT or PPARγ-WT; $^{\#}p < 0.05$, $^{\#\#}p < 0.01$, and $^{\#\#\#}p < 0.001$ versus RXRα-WT or PPARγ-WT treated with RSG or 9cRA. Data are represented as means ± SEM from at least three mice per genotype. *D*, PPARγ binding in macrophages in relation to several genes involved in phagocytosis, as they appear in the mm8 Mouse Genome Assembly (2006) in the USCS Genome Browser (http://genome.ucsc.edu). In blue are PPARγ-significant ChIP-seq binding regions with an FDR of 0.5%. In red is a version of the dataset using an FDR of 5%. Also shown in black are ChIP-seq results for H3K9Ace in macrophages.

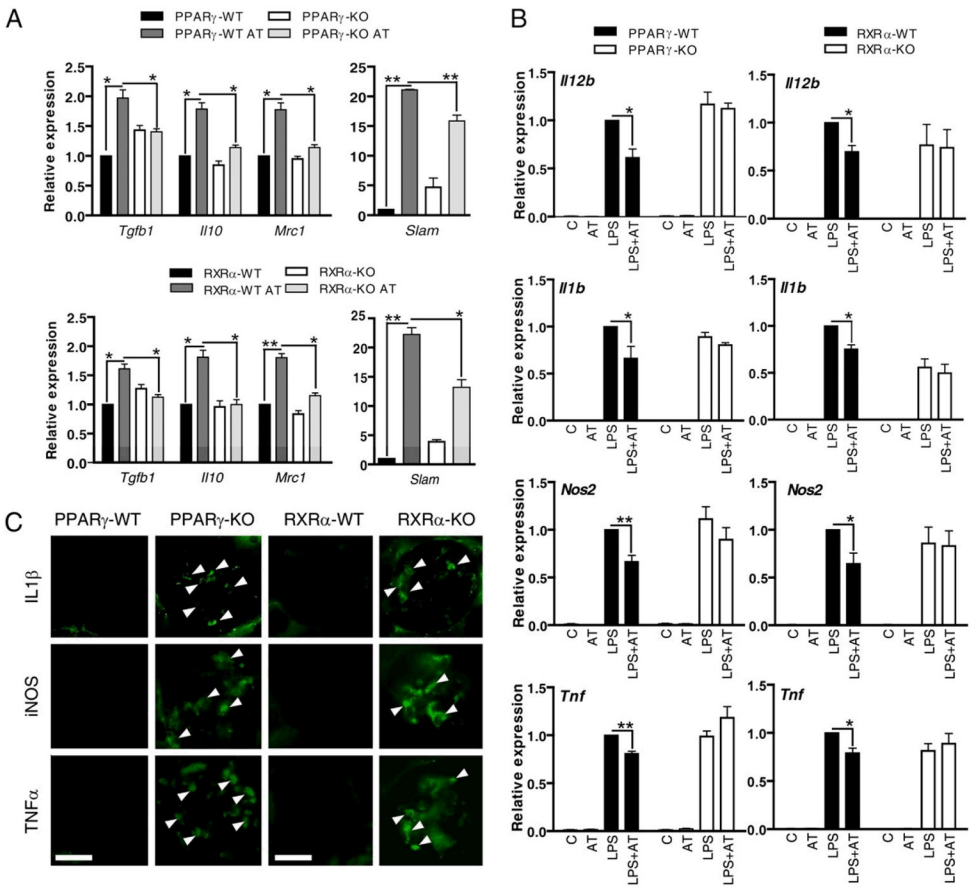

FIGURE 5.

Apoptotic cells cannot reduce proinflammatory gene transcription in PPARγ-KO and RXRα-KO macrophages. *A*, Macrophages were incubated for 24 h with ATs, and transcript levels of *Tgfb1*, *Il10*, *Mrc1*, and *Slam* were analyzed. *B*, WT, PPARγ-KO, and RXRα-KO macrophages were preincubated with ATs for 30 min and then challenged with 100 ng/ml LPS for 5 h. Transcript expression of proinflammatory genes was quantified by real-time PCR and expressed as the fold induction relative to LPS treated WT cells. Data are represented as means ± SEM from at least three mice per genotype. *$p < 0.05$; **$p < 0.01$. *C*, Immunohistochemical detection of inflammatory markers (IL1β, iNOS, and TNF-α) in kidney sections of 4–6-mo-old mice. Arrowheads indicate positively-stained inflammatory cells within the glomeruli. Scale bar, 35 μm.

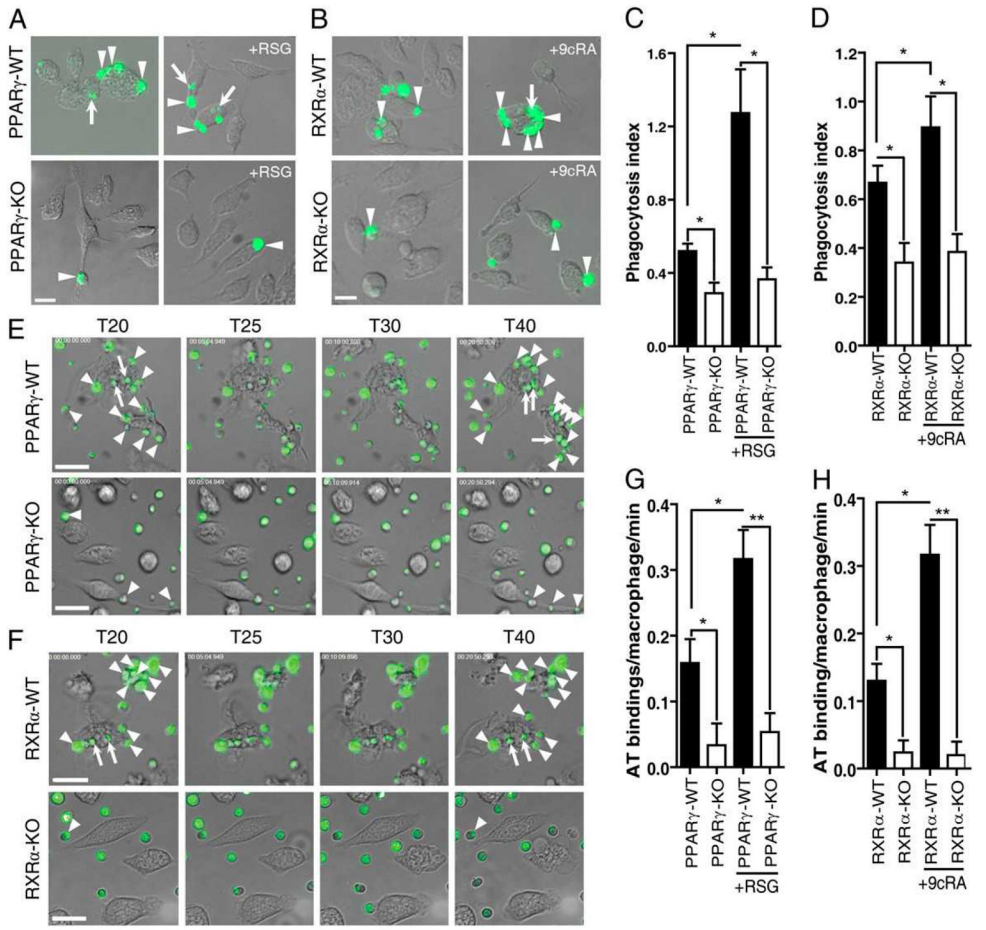

FIGURE 6.

Apoptotic cell uptake in vitro is impaired in PPARγ-KO and RXRα-KO macrophages. *A* and *C*, In vitro uptake of fluorescently-labeled ATs by WT and PPARγ-KO peritoneal macrophages. Arrowheads indicate ATs attached to macrophage filopodia; arrows indicate ingested ATs. Images were obtained 60 min after exposure of macrophages to labeled ATs. Phagocytosis index is the number of ingested ATs per macrophage. *B* and *D*, In vitro uptake of fluorescently labeled ATs by WT and RXRα-KO macrophages. *E* and *F*, Real-time analysis of phagocytosis reveals a reduced ability of PPARγ-KO and RXRα-KO macrophages to bind ATs. Images were obtained 20–40 min (T20–T40) after exposure of macrophages to labeled ATs. Arrowheads indicate attached ATs; arrows indicate ingested ATs. Scale bars, 5 μm. *G* and *H*, Quantification of AT binding. All tests were performed on macrophages isolated from six mice per genotype. Data are represented as mean values ± SEM. To test the effects of PPARγ and RXRα ligands, macrophages were treated with 1 μM RSG or 100 nM 9cRA for 18h. *$p < 0.05$; **$p < 0.01$.